Materials Research. 2018; 21(1): e20170189
DOI: http://dx.doi.org/10.1590/1980-5373-MR-2017-0189

Effect of Urea Excess on the Properties of the $MgAl_2O_4$ Obtained by Microwave-Assisted Combustion

Luciene Santos Carvalho[a,b]*, Vitor Rodrigo de Melo e Melo[a], Eledir Vitor Sobrinho[a], Doris Ruiz[c], Dulce Maria de Araújo Melo[a]

[a]*Universidade Federal do Rio Grande do Norte, Campos Lagoa Nova, 59078-970, Natal, RN, Brazil*
[b]*Instituto Federal da Bahia, Loteamento Espaço Alpha, s/n, BA 522, Limoeiro, 42802-590, Camaçari, BA, Brazil*
[c]*Departamento de Físico Química, Facultad de Ciencias Químicas, Universidad de Concepción, Campus Concepción, Edmundo Larenas, 129, Casilla 160-C, Concepción, Región del Bio Bio, Chile*

Received: February 09, 2017; Revised: August 20, 2017; Accepted: September 17, 2017

In this paper, magnesium aluminate spinels were prepared by microwave-assisted combustion, using urea as fuel. In order to evaluate the effect of the urea excess used in the synthesis, its mass was added in a range of 1.0 to 2.5 times the stoichiometric amount required. The materials produced were characterized by TGA, FTIR, XRF, XRD, BET, SEM and TEM. The results demonstrated that magnesium aluminate spinel was formed in all solids, but the crystallinity degree and the specific surface area increased according to the amount of urea that was used in the synthesis. The use of excess fuel in the preparation was therefore advantageous, since it eliminated the need of the calcination step, at high temperatures, in order to stabilize the spinel phase and improve the crystallinity of the solid. The heat generated in the combustion process was sufficient to develop the formation of a nanocrystalline structure and produce high purity materials, with a save of 99.4% in energy.

Keywords: *Microwave Synthesis, Nanocrystals, Structural Properties, $MgAl_2O_4$, DRX*

1. Introduction

The magnesium aluminate, $MgAl_2O_4$, is a typical spinel with a crystalline structure AB_2O_4, where A is a bivalent metal cation at a tetrahedral site and B is a trivalent metal cation at an octahedral site of the cubic structure[1]. Due to its low density (3.56 g cm^{-3}) and acidity, high melting point (2135 °C), chemical attack resistance, mechanical resistance at high temperatures, excellent optical properties, low thermal expansion coefficient and dielectric constant[1-3], sintering resistance and good interaction with the active phase $MgAl_2O_4$ has numerous industrial and technological applications. For example, this material has been used as support for metal catalysts to methane reform[4,5], decomposition of methane[6], dehydrogenation of n-butane[2], ethanol reforming[7,8], Fischer-Tropsch reaction[9], among other processes. For applications such as catalytic support the solid must have a high surface area, usually obtained from small size particles, or low area, associated with high porosity and mechanical resistance, which allows its use as a catalyst carrier[10-12]. Thus, to choose the synthesis and processing methods for these materials is very important.

There are several processes to prepare nanocrystalline magnesium aluminate, such as sol-gel[13-16], co-precipitation[17], complexation[1,18], mechanical milling[3], mechanical-chemical process[19], hydrothermal[20], micro emulsion[21], combustion method[15,22-26] and fast pyrolysis[27]. However, many of those are complex, expensive, have several steps, require long time for synthesis, require high temperatures and produce non-homogeneous and generally low surface area solids[28]. In the case of solution combustion method, it has been extensively used recently, due to its several advantages, such as simplicity, low cost, short synthesis time and less amount of external energy required, also it produce powders of oxides more homogeneous, more crystalline and of higher purity[29-31]. This technique basically consists of using aluminum and magnesium nitrates as oxidants and an organic compound (urea, glycine, sorbitol, citric acid, among others) as fuel. It is the heat generated during the combustion reaction between oxidant and fuel (reducing agent) that promotes the formation of the material[28,29,32]. A large amount of gases (CO_2, NO_x, N_2, H_2O, CO) are also released during the process, and is responsible for the destruction of agglomerates and the formation of micropores in the material, facilitating the access of reagents to the active sites[31,32], if the spinel is used as catalyst support.

It has been discovered that microwave irradiation can also be used for the synthesis and sintering of ceramic materials by combustion, being a quicker and more effective way when compared to the use of conventional oven. This is because, unlike what happens in the conventional oven, where the warm comes from external sources, in microwave the heat is generated inside the material. As a consequence,

*e-mail: prof.lucarvalho@gmail.com

the process happens very fast and the entire volume of particles is uniformly warming, since the penetration depths of radiation are generally high. This minimizes the formation of thermal gradients[33]. Due to the advantages presented by microwave-assisted combustion[34,35], many researchers have used the technique in the synthesis of materials for various applications[32,36-38], including obtaining of nanocrystalline $MgAl_2O_4$[3,30,39,40].

When synthesizing spinel powders of $MgAl_2O_4$, from a mixture of the precursors solid such as aluminum nitrate, magnesium nitrate and urea, Ganesh et al.[30] compared the routes of conventional combustion and microwave-assisted combustion. They concluded that the microwave preparation was more advantageous, since the powders had crystals in the range of 20-50 nm, while by conventional oven combustion the powders obtained were presented as agglomerates of fine crystals, in the range of 100-250 nm. Bai et al.[39] performed the synthesis of $MgAl_2O_4$ powders by microwave-assisted combustion using various mixtures of the fuels such as starch, urea and glycine. They observed that as the starch content increased in the blend, there was a decrease in crystallite size and an increase in the specific surface area of the solid as a consequence of the higher amount of gases released during the process. On the other hand, Medeiros et al.[40] evaluated the influence of synthesis parameters by microwave-assisted combustion, such as fuel/oxidant ratio, microwave power and calcination temperature of the $MgAl_2O_4$ powder structure. According to these authors, in order to form $MgAl_2O_4$ with a higher degree of crystallinity and a smaller crystallite size, the combustion reaction must be performed with a fuel/oxidant ratio less than 1:1, with the microwave operating at a power greater than 675 W, and after the synthesis realizing a calcination at 900 °C. However, in most papers, the authors used long preparation times or high calcination temperatures to obtain the materials, or started from the mixture of the solid precursors on the combustion stage.

Once that Medeiros et al.[40] used fuel/oxidation ratios equal to 0.8, 1.0 and 1.2 for the material synthesis and did not evaluate the influence of use a higher amount of urea during the preparation, this paper intends to investigate the effect of urea in excess on the synthesis by microwave-assisted combustion on the textual and structural properties of $MgAl_2O_4$. In order to do that, during the syntheses process, a mass of urea from 1.0 to 2.5 times the stoichiometric amount required was added, and the materials obtained were characterized by TGA, FTIR, XRF, XRD, BET, SEM and TEM.

2. Materials and Methods

2.1 Samples preparation

The stoichiometric mass of the magnesium nitrate ($Mg(NO_3)_2.6H_2O$, SIGMA-ALDRICH, purity ≥ 98%) and aluminum nitrate ($Al(NO_3)_3.9H_2O$, SIGMA-ALDRICH, purity ≥ 98,5%) precursors required to obtain $MgAl_2O_4$ was weighted, and sequentially it was added to a beaker containing 15 mL of water together with the urea (CH_4N_2O, VETEC). The determination of the nitrates masses as well as of the fuel, the urea, were made on the basis of the chemical knowledge of the propellants and explosives, as it was described by Ganesh et al.[30]. According these authors, to synthesize magnesium aluminate spinel by combustion route with urea (total valencies +6), employing $Al(NO_3)_3.9H_2O$ (total valencies -15) and $Mg(NO_3)_2.6H_2O$ (total valencies -10) as sources of Al and Mg, respectively, it can be determined the urea amount required to balance the total oxidizing and reducing valencies in the mixture by direct use of propellant chemistry criterion, which leads to the equation: $1(-10)+2(-15)+n(+6)= 0$. In this way, the stoichiometric redox mixture of Al and Mg nitrates and urea, to release the maximum energy for the combustion reaction $2\ Al(NO_3)_3.9H_2O(c)+Mg(NO_3)_2.6H_2O(c)+6.66\ CH_4N_2O(c) \Leftrightarrow MgAl_2O_4\ (c)+ 6.66\ CO_2\ (g)+(4+6.66)\ N_2\ (g)+(24+6.66 \text{ x } 2)\ H_2O\ (g)$, where (c) is crystalline and (g) is gas, would require n = 6.66 mol. Therefore, the masses of urea used were 1.0, 1.5, 2.0 and 2.5 times the stoichiometric quantity (~400 g), calculated from n value determined as described by Ganesh et al.[30], divided by a factor that led to obtaining 1-2 g of magnesium aluminate. After the complete dissolution of the reactants, under continuous heating for 20 min and constant stirring, the concentrated solution was submitted to microwave radiation in a conventional house microwave that was adapted for synthesis, and adjusted to a power of 675 W for 10 min. The blast occurred in less than 3 min, with a white smoke released, the formation of a flame, and finally of a spongy white solid. The materials were carefully collected and triturated, and the powders obtained were not submitted to drying or calcination steps. The prepared samples were identified as MA0U, MA50U, MA100U and MA150U, where MA stands for magnesium aluminate, and the numbers indicate the percentages of excess urea that was used. In order to evaluate the effect of the calcination on the loss of mass and on the crystallinity of the material, the sample MA0U was calcinated with air flow at 900 °C for 4 h, obtaining the sample MA0UC900.

2.2. Samples characterization

The thermogravimetric analyzes (TGA) of the solids were performed on a Q600 V20.9 SDT equipment, TA Instruments, under N_2 atmosphere in a range of 10-900 °C, with heating rate of 10 $^{o}min^{-1}$. In order to identify the formation of magnesium aluminate spinel in the samples, Fourier transform infrared (FTIR) absorption spectrum was recorded employing a spectroscope model IRPrestige-21, from SHIMADZU. The powders of the samples were mixed with KBr and then compressed into a pastille form. The scanning was performed in the range of 400 to 4000 cm^{-1}. The chemical analysis of materials for the determination of magnesium and aluminum

contents was performed by X-ray fluorescence (XRF) on a Shimadzu EDX-720 instrument. The X-ray diffractograms (XRDs) were obtained from a Shimadzu equipment, model XRD7000, using CuKα radiation (0.154 nm). The data was collected in a range of 10 to 80º. The specific surface area of the solids was determined from isotherms of physical nitrogen adsorption at -196 ºC in a TriStar II 3020 equipment from Micromeritics. Before analyzes, the samples (100 mg) were heated under vacuum at 120 ºC for 3 h. The specific surface area values were measured by the Brunauer-Emmett-Teller method (BET), while the pore size distribution was calculated from desorption curve by the Barrett-Joyner-Halenda (BJH) method. The morphologies of the samples were compared by means of scanning electron microscopy (SEM) images on a VEGA 3 equipment, from Tesca, operating at 15 kV. Transmission electron microscopy (TEM) images of the samples, previously dispersed in ethanol, were also obtained using Jeol JEM 1200 EXII equipment. The distribution of particle sizes was done counting only the structures with defined edges, and not larger than 140 nm. TEM images were analyzed using an Image Tool 3.0 program. The particles were counted manually to minimize the error due to the automatic analysis, and the later quantification was made using the Gaussian function of the Origin program.

3. Results and Discussion

Thermogravimetric curves of the samples obtained from the microwave-assisted combustion synthesis, using different urea contents, are shown in Fig. 1a. Three regions of mass loss were identified, which can be seen more clearly by the DTG curves in Figure 1b. The first (50-150 ºC) and the second (160-330 ºC) region are related to evaporation of the adsorbed moisture and the decomposition of part of the aluminum nitrate, while the third region between 350 and 580 ºC can be attributed to the decomposition of aluminum nitrate and of magnesium nitrate that not reacted[9,11]. The results are in accordance by Halabi et al.[25], which identified one weak mass loss event at 136 ºC related to adsorbed residual water, and two strong mass loss events in the 136 ºC-306 ºC and 306 ºC-540 ºC temperature ranges. These regions of mass loss are not present in the profiles of samples MA100U and MA150U, indicating that the combustion of nitrates was completed when an excess of urea above 100% was used during the reaction. It was also observed that there was a decrease in mass loss of the samples as a function of temperature as the amount of urea that was used in the combustion process increased. The values of total mass loss of the samples were located in the range of 3-25%, been the highest value related to the sample prepared without excess urea (MA0U), and the lowest value was observed for the sample obtained with the use of 150% excess of urea (MA150U).

In order to observe the effect of calcination on mass loss was also obtained the thermogravimetric curve of the sample prepared without excess urea, calcined at 900 ºC for 4 h (MA0UC900). From the profiles shown in Fig. 1a, it was noted that, in the case of the non-calcined sample (MA0U), the loss of mass was about 25% and, after calcination (MA0UC900), the mass loss was insignificant, around 2.3%, probably due to evaporation of the moisture from the atmosphere, which was absorbed by the material. No event of mass loss was observed on the DTG curve of this sample, showed in Fig. 1b. It is interesting to note that the mass loss of the MA0UC900 sample was similar to that of the MA150U sample, which was prepared using excess of 150% of urea, that is, when using an excess of fuel, the calcination step can be dispensed. In this way, a material with high thermal and compositional stability is obtained,

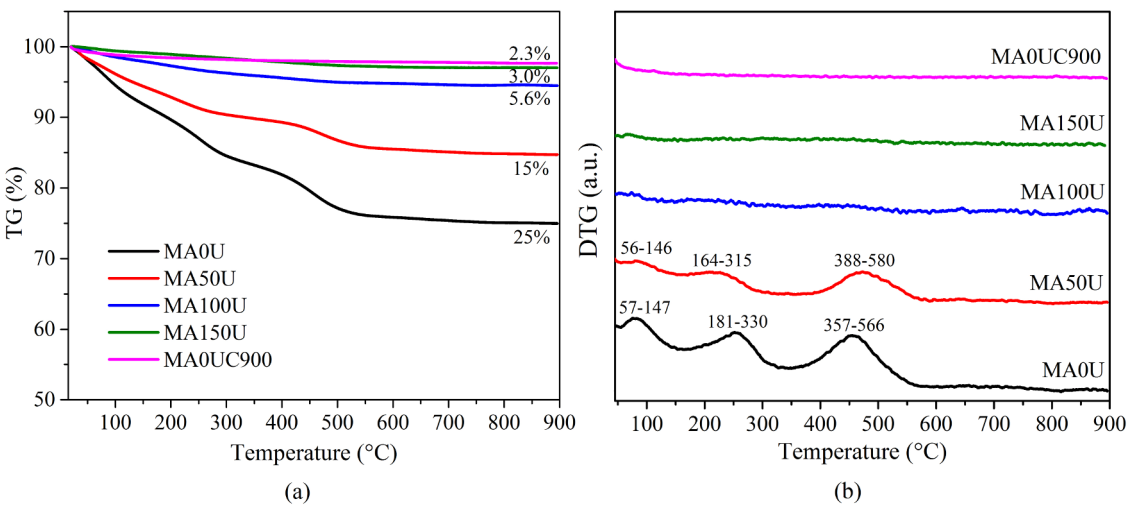

Figure 1. TG (a) and DTG (b) of the samples obtained without the use of urea excess, not calcined (MA0U) and calcined at 900 °C (MA0UC900), and with the use of 50% (MA50U), 100% (MA100U) and 150% (MA150U) of urea excess.

as it was observed by other authors who used the method of microwave-assisted combustion[30].

The bands that corresponding to the vibrations of the Al-O bonds of the octahedral AlO_6 groups[42], and to the network vibrations of Mg-O bonds[43], which appear in the region of 700-510 cm^{-1} of the FTIR spectrum shown in Fig. 2a, are typical of the spinel structure of magnesium aluminate[3,16,19,24,27,28]. In a recent work, Erukhimovitch et al.[24] detected four main vibrations modes (γ_2, γ_1, γ_5 and γ_6) at about 523, 692, 828 and 910 cm^{-1} in the FTIR spectrum of stoichiometric magnesium aluminate spinel. Modes in γ_2 and γ_1 occurred in similar frequency values to those found in this work and were also assigned to vibrations of the trivalent cation (Al^{3+}) located in the octahedral sites. It confirmed that there was also formation of stoichiometric magnesium aluminate spinel in all samples obtained in the present study. The shoulder observed at about 800 cm^{-1} is consistent with the hypothesis that some Al^{3+} ions also occupy tetrahedral positions in the spinel formed[27]. It was observed that all spectra showed very similar profiles, in which bands with absorption maxima around 3500 cm^{-1} and 1650 cm^{-1} were identified, attributed to the stretch vibrations of O-H groups, and of H-O-H molecules deformation of the water physically adsorbed and in interaction with $MgAl_2O_4$, respectively[3,19,28]; an absorption band at about 2339 cm^{-1}, referring to the stretch vibration of C=O bond of the carbon dioxide from the air[27]; in addition to the band with the maximum absorption, around 1370 cm^{-1}, attributed to the vibrations of the N-O bond of NO^{3-} groups. The division of the high-frequency band into two can be explained by considering that a number of Al^{3+} ions occupy the sites in the spinel type structure, as indicated to Edwais et al.[44]. When the FTIR spectrum of the four samples (Fig. 2a) is compared, it is possible to note that there is a deepening of the absorption peaks that are related to the Mg-O-Al bonds, which increase in intensity from the MA0U sample to the MA150U sample. The FTIR spectrum also show that a smaller amount of water and residual nitrate is present in the samples prepared with the use of 100% (MA100U) and 150% (MA150U) of urea excess during combustion. These facts indicate that, as the amount of urea used in the synthesis by microwave-assisted combustion increases, the formation of $MgAl_2O_4$ spinel becomes more complete, and the solid obtained is purer and more crystalline.

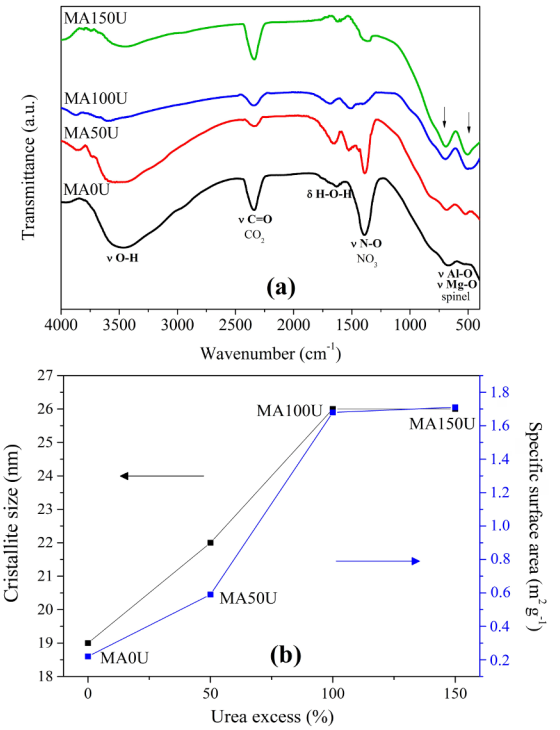

Figure 2. (a) FTIR spectra of the samples. (b) Crystallite sizes (XRD) and specific surface area (BET) of the solids, in function of the urea excess.

XRF analyzes data, performed with two of the samples and shown in Table 1, also confirm the formation of the $MgAl_2O_4$ structure, once that, considering the detection limits of the technique, the contents values of Mg and Al present in the samples (real value) are in accordance with the nominal values of the metals in the $MgAl_2O_4$ spinel of stoichiometric composition. The produced materials were free of organic compounds, as it can be observed by FTIR and XRF results, and XRD results that be discussed subsequently.

Diffraction patterns of the synthesized powders from the use of different amounts of urea in the combustion are shown in Fig. 3. In all profiles, the presence of the magnesium aluminate ($MgAl_2O_4$) spinel phase was identified, which belongs to the cubic system and Fd-3m space group. Its

Table 1. Values of: metal contents, specific surface area (Sg), pore volume (Pv), average pore diameter (Pd), particle size (Ps), calculated from (BET), crystallinity degree (Cd), crystallite size (Cs), determined by XRD and TEM.

Sample	Metals content (%)				Sg (m^2g^{-1})	Pv (cm^3g^{-1})	Pd (nm)	Ps (BET) (μm)	Cd (%)	Cs (DRX) (nm)	Cs (TEM) (nm)
	Nominal		Real								
	Mg	Al	Mg	Al							
MA0U	31	69	29	71	0.22	-	-	7.7	44	19	31
MA50U	-	-	-	-	0.60	-	-	2.8	47	22	32
MA100U	-	-	-	-	1.68	0.002	28	1.0	75	26	33
MA150U	31	69	29	71	1.71	0.002	29	1.0	79	26	37

main reflections values are present in 2θ equal to 19.0, 31.2, 36.8, 44.7, 55.6, 59.3, 65.1 and 77.2, corresponding to the crystalline planes (111), (220), (311), (400), (422), (511), (440) and (533), respectively (JCPDS 01-075-1797 card). Similar X-ray diffractograms were obtained by other authors[13,16,18,21,24-26,30,39,40,44].

Comparing the profiles of the samples shown in Fig. 3, it can be seen that more defined and with higher intensity peaks were obtained as the amount of urea used during the synthesis by microwave-assisted combustion was increased. That is, the crystallinity of the magnesium aluminate increased with the urea content, and the most crystalline material was the one synthesized with 150% excess urea (MA150U). The crystallinity degree values (Cd) of the obtained solids, determined from the equipment used in the XRD analyzes, can be compared from the data in Table 1.

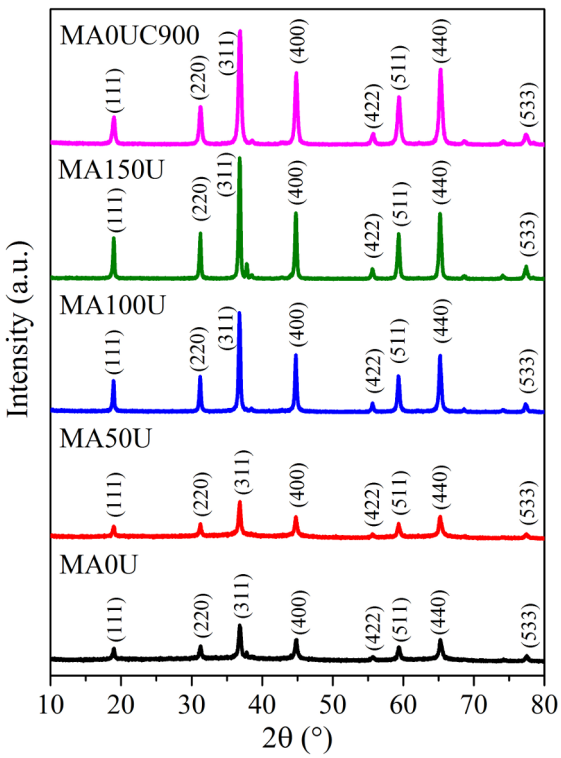

Figure 3. XRD of the samples obtained by using distinct quantities of urea during the synthesis.

From Fig. 3 it is also possible to note that, when no excess urea is used in the synthesis (MA0U), a less crystalline material is obtained, so that more defined and more intense peaks are observed after the calcination of the solid at 900 ºC (MA0UC900). However, the spinel prepared from the combustion using 150% of urea excess (MA150U) showed a diffraction pattern corresponding to a material with higher crystallinity, even without realize the drying or calcination steps after the reaction in the microwave.

The average crystallite size of the solids was estimated from the X-ray patterns, using the Scherrer equation and applying the integral width method, defined as the total area under the maximum diffraction peak divided by the peak intensity[45]. The diffraction peak that was considered in the calculations was the one corresponding to the plane (311), which occurs at 2θ = 36.8. A well-known expression of the Scherrer formula was used to determine the average size of the crystallite, L, and can be seen in (1):

$$L = \frac{K\lambda}{\beta \cos\theta} \quad (1)$$

where λ is the length of the radiation (in this case, CuKα = 0.154 nm); θ is the angle corresponding to the point of the highest intensity diffraction peak; *K* is an instrumental constant that depends on the shape of the crystallite, which value is considered unitary in the calculation method applied; and β is the integral width of the maximum diffraction peak, which can be determined by using expression (2):

$$\beta = \frac{\int_{2\theta_1, I(2\theta_1)=0}^{2\theta_2, I(2\theta_2)=0} I}{I_{max}} \quad (2)$$

in that $2\theta_1$ and $2\theta_2$ are the values of 2θ at the initial and final of the highest intensity peak (I) and I_{max} is the intensity value at the maximum point of the diffraction peak.

Fig. 2b presents a correlation between the crystallite sizes, the specific surface area of the samples obtained and the excess of urea used in the preparation of the materials by microwave-assisted combustion. The graphic shows that increasing the content of urea during the microwave-assisted combustion process result in an increase of the crystallite size of the material. The smaller size was 19 nm when was used the quantity stoichiometric of urea, while crystallites of about 26 nm were formed when 100% of urea excess was used in the synthesis. These results are in accordance with the ones from the XRD patterns, in which was observed a narrowing of the peaks was found in the profiles of samples MA100U and MA150U, showing that when it is used at least twice the stoichiometric quantity of urea in the synthesis by microwave-assisted combustion, materials with high crystallinity and purity are obtained without the need for subsequent thermal procedures. This means time savings and energy during the preparations.

The average crystallite sizes obtained in this work were of the same order as those of the nanocrystalline $MgAl_2O_4$ synthesized by Rashad et al.[46] (25 to 33 nm), which used the co-precipitation method and calcination at 600 to 800 ºC. On the other hand, the values were smaller than the obtained by Erukhimovitch et al.[24] (60 nm), which has synthesized stoichiometric $MgAl_2O_4$ spinel by a conventional combustion method, using citric acid as a fuel, or by Torkian et al.[47] (75 nm), which prepared stoichiometric nanoparticles of $MgAl_2O_4$ spinel by microwave assisted combustion of an aluminum nitrate nanohydrate and magnesium hydroxide

mixture in stoichiometric amount, in the presence of urea as a fuel and using about 20 min of irradiation.

All samples presented low values of specific surface area, ranging from 0.2-1.7 $m^2 g^{-1}$, as it is shown in the graph on Fig. 2b. However, it was possible to observe that, with the increase of the excess of urea used in the synthesis, there was an increase in the value of the specific area, until the use of 100% excess of urea. Thereafter, no further change in the specific surface area of the material occurred. It is also interesting to emphasize that, according to the materials obtained and the methodology employed in this paper, an increase in crystallite size also resulted in an increase in specific surface area. In this case, it was confirmed that, in fact, "crystallite size" is not a synonymous for "particle size", as it is emphasized by other authors[45,48], once that the individual particles may contain several crystallites[41]. In addition, it is well known that the specific surface area and particle size values have an inverse relation to each other, which can be represented by Eq. (3), where S is the specific surface area (BET), 6 is a constant that is used when a spherical geometry of the particles is considerate, ρ is the specific mass of the compound and d is the particle size[49,50]. In other words, small particle sizes result in high specific surface area values. The values of the crystallite size, as determined by XRD, and particle size may coincide when the particle is constituted of one single crystal, which can occur with very fine powders, of materials with high specific surface area. In this case, under the conditions of surface area measurement by BET, the N_2 gas will be adsorb by the surface of single crystals and therefore an inver se correlation will be found between the values of specific area and crystallite sizes.

$$S = \frac{6}{\rho.d} \quad (3)$$

Using Eq. (3), although the particles do not present a spherical geometry, it is possible to estimate the average particle size values of the synthesized materials in order to infer, in a comparative way, about the effect of fuel excess used in synthesis on textural properties of the materials. The obtained data, expressed in Table 1, showed that there was a reduction in particle size with the increase of the amount of excess urea used in the microwave-assisted combustion. Samples that were prepared using 100% (MA100U) or 150% (MA150U) of excess urea presented smaller particles, about of 1.0 μm, while the synthesis with stoichiometric quantity of urea led to the solid with the largest value of average particle size (7.7 μm). Therefore, using at least twice the mass of urea required for synthesis by microwave-assisted combustion brings benefits to the textural and structural properties of the material.

It was identified the absence of hysteresis in the nitrogen adsorption and desorption isotherms of the obtained solids, as it can be seen by the curves of samples MA100U and MA150U shown in Fig. 4. This not mean absence of porosity, but that the formats and sizes of pores presented by the samples may be leading to similar adsorption and desorption processes. Since the AM0U and AM50U samples presented very low and insignificant specific surface area values (Table 1), and their isotherms did not show a typical format of materials with porosity in the known classes, it was not possible to determine the pore volume and the average pore diameter value. On the other hand, the adsorption isotherms of the samples MA100U and MA150U were similar, presenting a typical Type II profile, characteristic of non-porous materials, macroporous or with diameters superior to those from micropores (Dp < 2 nm). However, from the pore size distribution of samples MA100U and MA150U, shown in Fig. 4, the presence of macropores (Dp > 50 nm) in the analyzed powders was not identified. For these samples, the pores are in the mesopores class (2 nm < Dp <50 nm), with diameters ranging from 10 to 35 nm. The average pore size was 28-29 nm and the total pore volume value was about to 0.003 $cm^3 g^{-1}$ (Table 1).

Morphologies of the samples showed similarities, as it can be seen by the SEM images of MA0U and MA150U samples (Fig. 5). The particles of the solids presented a format of thin sheets or plates with an irregular geometry and size, which is in accordance with the results obtained by Medeiros et al.[40]. However, it was possible to notice that the particles from the sample MA0U presented a more smooth and homogeneous appearance, appearing a low porosity. On the other hand, the particles of the sample MA150U showed an appearance more rough and porous. These differences are a consequence of the use of distinct fuel masses, urea, during the synthesis by microwave-assisted combustion. When an excess of 150% of urea was used, a greater amount of gases was released during the reaction, causing the formation of void spaces and porosity on the surface of the solid. This also explains the highest specific surface area value of the sample MA150U, which was about eight times greater than that of the sample MA0U. From the SEM images, it is also possible to note that the particles size of the materials varied widely with grains ranging from below 2 μm to above 100 μm. That is, the particles of the obtained materials are large and composed of smaller crystals agglomerates. Hence, the considerable difference between the crystallite sizes determined by XRD and the grain sizes, estimated by BET (Table 1).

Comparing the TEM images of solids prepared from the use of different masses of urea during the microwave-assisted combustion (Fig. 6), it can be identified that the plates observed by SEM are, in fact, constituted by an agglomerate of smaller dimensionally particles presenting irregular sizes and shapes. A smaller degree of agglomeration was observed in the image of the sample synthesized with 150% urea (MA150U), which is in accordance with BET data. The decrease in the quantity of particles agglomerates

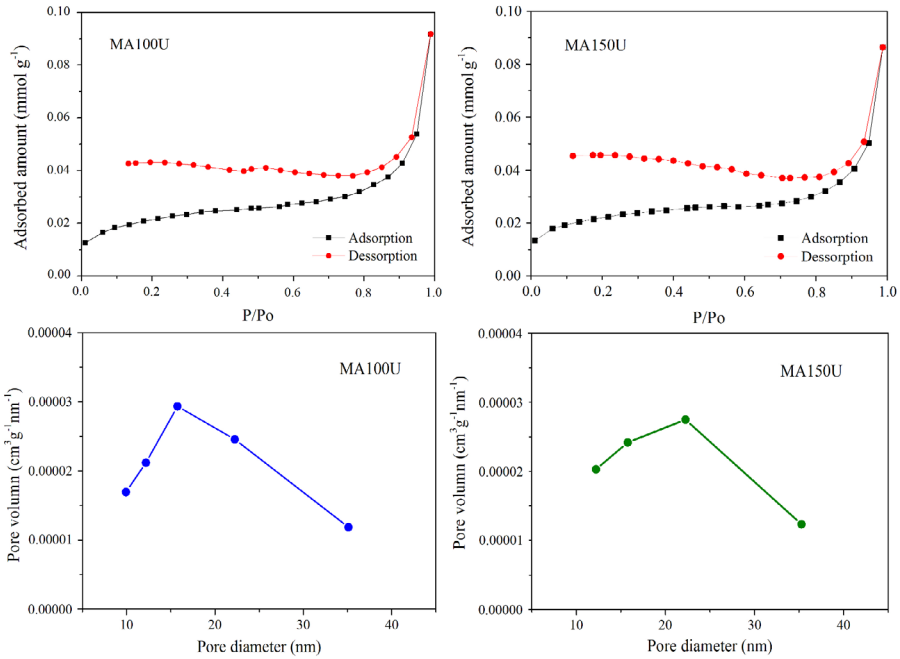

Figure 4. Nitrogen adsorption and desorption isotherms and pore size distribution of the MA100U and MA150U samples.

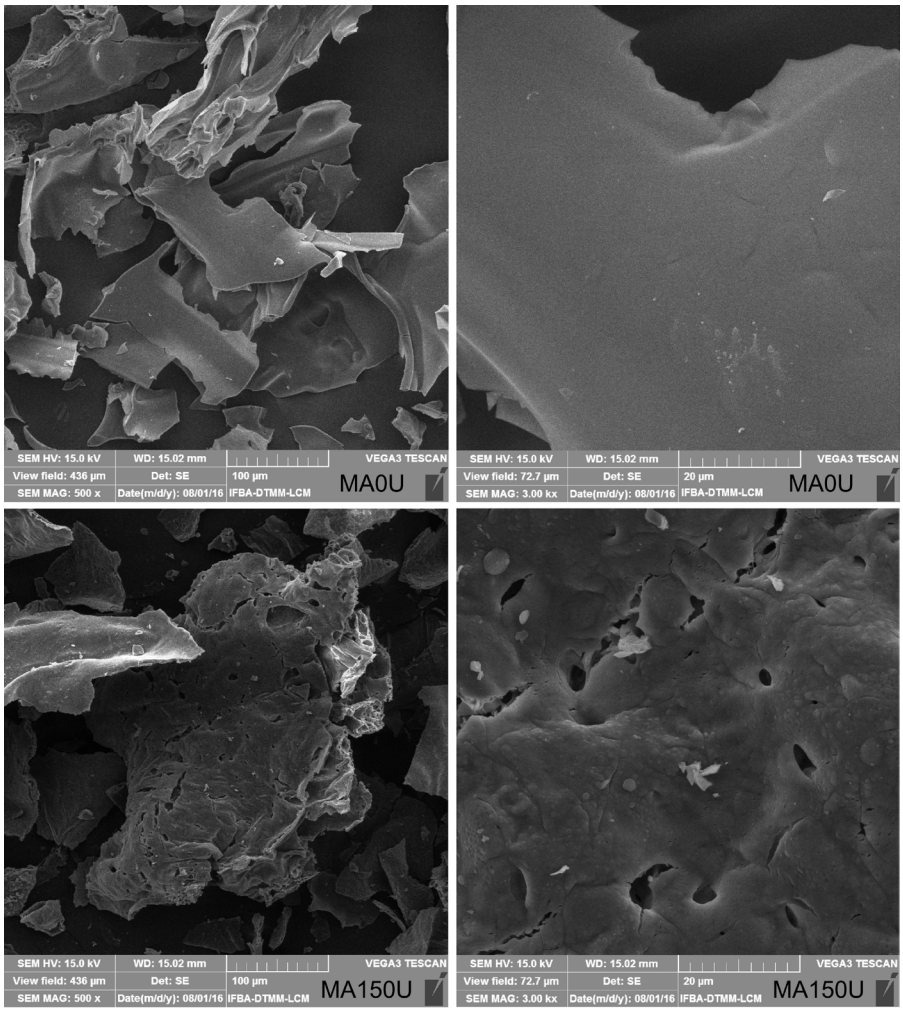

Figure 5. SEM images of the MA0U and MA150U samples, with different magnification.

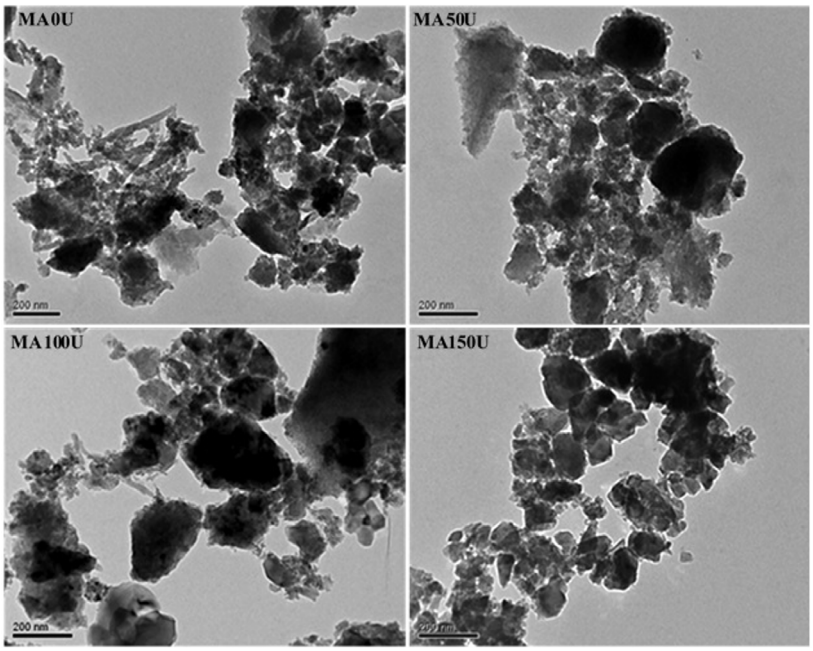

Figure 6. TEM images of the samples prepared from the use of distinct masses of urea during the microwave assisted combustion.

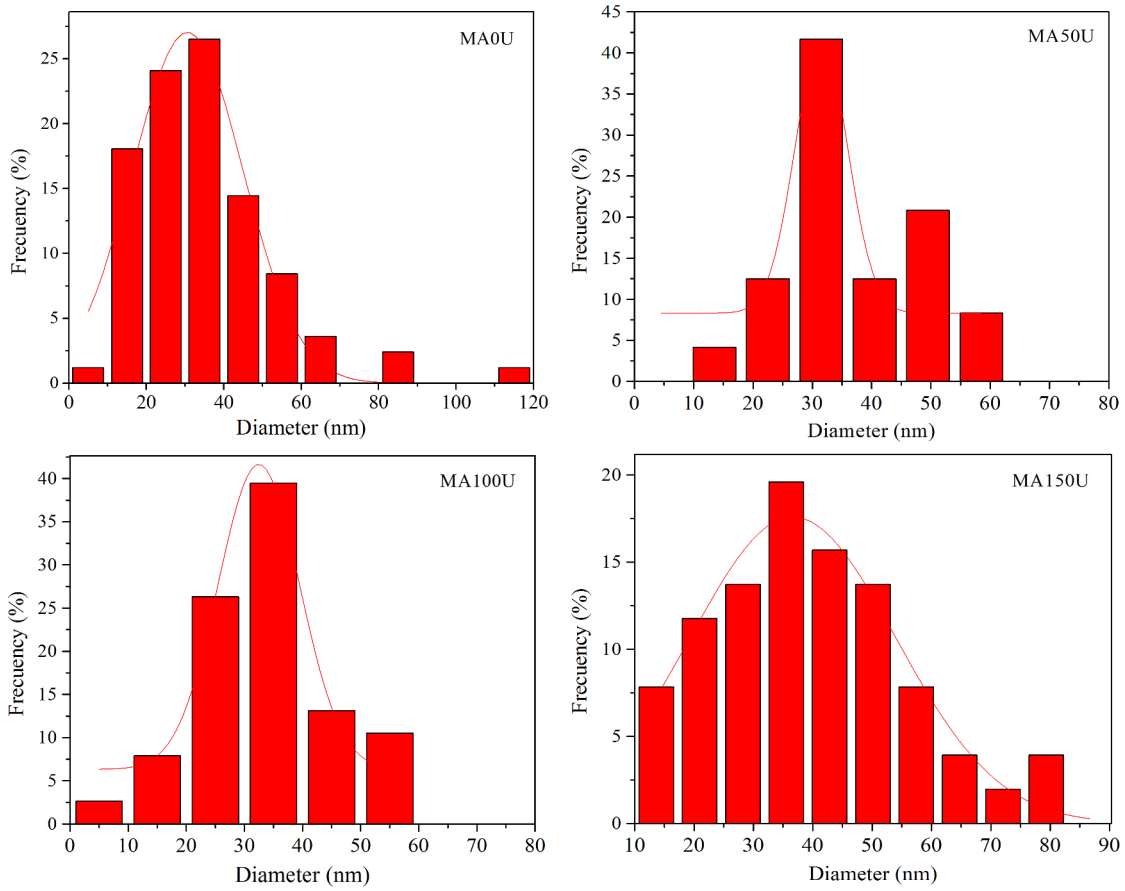

Figure 7. Crystallite size distribution of the samples prepared from the use of distinct masses of urea during the microwave assisted combustion.

is a consequence of the higher release of gases during the combustion process when excess urea is used, as it was discussed previously.

The particles with defined edges and diameters up to 140 nm, present in the TEM images of the four samples on Fig. 6, were counted, and the data was organized into statistical graphics of crystallite size distribution, which are shown in Fig. 7. One can observe that for all samples the diameter is generally an increasing function of the urea excess used in the preparations. The histograms show a narrower crystallite size distributions profile for the sample prepared with lower urea concentration. Higher counts of crystals were observed in the range of 10 to 70 nm. On the other hand, the Gaussian distribution was the amplest for the sample MA150U. In short, the more urea excess was added during the materials synthesis, more of crystallite population was shifted for higher diameters values, and the crystallinity of the solids increased, as confirmed by XRD results.

The average crystallite size values of the solids, determined by TEM (Table 1) presented the same tendency of the crystallite sizes calculated from the XRD data (Table 1), that is, the higher the amount of urea used in the reaction, the greater the crystallite size of the magnesium aluminate obtained. However, the values were not equal, since an exact correlation between the crystallite sizes obtained by the two techniques would be fortuitous, as it was pointed out by Jiang et al.[51]. In recent studies[24,26], non-stoichiometric magnesium aluminate spinel powders were prepared by solution combustion method and presented small and comparable crystallite sizes, estimated at 13-15 nm. It was observed by the authors an accordance between crystallite sizes estimated by XRD and those estimated based on TEM analysis. The discrepancies found by comparing these results with ours could be explained considering that grain size is sensitive to magnesium aluminate spinel stoichiometry, as suggested by the authors, or because of the different sample preparation methods employed.

4. Conclusions

Nanocrystalline powders of magnesium aluminate spinel were synthesized by the microwave-assisted combustion method using urea as fuel. In order to evaluate the effect of the amount of urea used during the preparation on the structural and textural properties of the obtained materials, several analyzes were carried out by means of different techniques, which allowed to conclude that:

(I) the use of different masses of the fuel, urea, in the synthesis of magnesium aluminate by microwave-assisted combustion, affects the final characteristics of the solid, so that a purer $MgAl_2O_4$ spinel, more crystalline, with a higher crystallite average size, smaller particle size, with a higher specific surface area and more porous is obtained when at least 100% urea excess is added to the solution that is containing the reagents prior to exposure to microwave radiation. A more homogeneous and crystalline material was obtained with the use of 150% of urea excess in the synthesis;

(II) the synthesis by microwave-assisted combustion demonstrated to be a fast and efficient method to obtain magnesium aluminate spinel with stoichiometric composition and stable. The use of at least 100% excess fuel in the process still provides an additional advantage, since the drying and calcination steps that occur at elevated temperatures, above 900 °C, which are normally required to obtain a material so crystalline, pure and stable as possible, can be dispensed, once the heat generated during the combustion is sufficient to stabilize the spinel phase and produce nanocrystals. As a consequence, energy is saved when calcination step is not performed. To estimate the amount of energy saved when using microwave assisted combustion, the following rough computation can be done: taking the set power of microwave oven (675 W) multiplied by the time of combustion process (3 min) is about 0.03375 kWh; while for the calcined material, taking the average power of the furnace used for calcination (1390 W) multiplied by the time of calcination process (4 h) one obtains an energy consumption of 5.56 kWh. Thus, the amount of energy saved is about 99.4%, which demonstrate the enormous advantage of the proposed technique.

5. Acknowledgments

The authors would like to thank to Conselho Nacional de Desenvolvimento Científico e Tecnológico - CNPq (Brazil), for the scholar grant issued to V.R.M.M, to PPGCEM/UFRN (Brazil), for the XRF analyzes, to LABTAM/UFRN (Brazil), for the TGA, FTIR and XRD experiments, to DTMM-LCM/IFBA (Brazil), for the SEM analyzes, and to Proyecto Fondo Nacional de Desarrollo Científico y Tecnológico - FONDECYT 1161660 (Chile), for the financial support.

6. References

1. Nuernberg GDB, Foletto EL, Probst LFD, Campos CEM, Carreño NLV, Moreira MA. A novel synthetic route for magnesium aluminate ($MgAl_2O_4$) particles using metal-chitosan complexation method. *Chemical and Engineering Journal*. 2012;193-194:211-214.

2. Bocanegra SA, Ballarini AD, Scelza OA, de Miguel SR. The influence of the synthesis routes of $MgAl_2O_4$ on its properties and behavior as support of dehydrogenation catalysts. *Materials Chemistry and Physics*. 2008;111(2-3):534-541.

3. Barzegar Bafrooei H, Ebadzadeh T. $MgAl_2O_4$ nanopowder synthesis by microwave assisted high energy ball milling. *Ceramics International*. 2013;39(8):8933-8940.

4. Guo J, Lou H, Zhao H, Chai D, Zheng X. Dry reforming of methane over nickel catalysts supported on magnesium aluminate spinels. *Applied Catalysis A: General*. 2004;273(1-2):75-82.

5. Hadian N, Rezaei M, Mosayebi Z, Meshkani F. CO_2 reforming of methane over nickel catalysts supported on nanocrystalline $MgAl_2O_4$ with high surface area. *Journal of Natural Gas Chemistry*. 2012;21:200-206.

6. Nuernberg GDB, Foletto EL, Campos CEM, Fajardo HV, Carreño NLV, Probst LFD. Direct decomposition of methane over Ni catalyst supported in magnesium aluminate. *Journal of Power Sources*. 2012;208:409-414.

7. Profeti LPR, Ticianelli EA, Assaf EM. Ethanol steam reforming for production of hydrogen on magnesium aluminate-supported cobalt catalysts promoted by noble metals. *Applied Catalysis A: General*. 2009;360(1):17-25.

8. Le Valant A, Garron A, Bion N, Epron F, Duprez D. Hydrogen production from raw bioethanol over $Rh/MgAl_2O_4$ catalyst Impact of impurities: Heavy alcohol, aldehyde, ester, acid and amine. *Catalysis Today*. 2008;138(3-4):169-174.

9. Rytter E, Holmen A. On the support in cobalt Fischer-Tropsch synthesis -Emphasis on alumina and aluminates. *Catalysis Today*. 2016;75:11-19.

10. Furimsky E. Hydroprocessing catalysts. In: Furimsky E. *Carbons and Carbon-supported Catalysts in Hydroprocessing*. RSC Catalysis Series. London: RSC Publishing; 2008. p. 12-21.

11. Choudhary VR, Banerjee S, Uphade BS. Activation by hydrothermal treatment of low surface area ABO_3-type perovskite oxide catalysts. *Applied Catalysis A: General*. 2000;197(2):L183-L186.

12. Boudjahem AG, Monteverdi S, Mercy M, Bettahar MM. Study of nickel catalysts supported on silica of low surface area and prepared by reduction of nickel acetate in aqueous hydrazine. *Journal of Catalysis*. 2004;221(2):325-334.

13. Heck AL, Taffarel SR, Hoffmann R, Portugal Jr UL, Jahn SL, Foletto EL. Síntese do espinélio $MgAl_2O_4$ via "sol-gel". *Cerâmica*. 2005;51(318):117-120.

14. Sanjabi S, Obeydavi A. Synthesis and characterization of nanocrystalline $MgAl_2O_4$ spinel via modi?ed sol-gel method. *Journal of Alloy and Compounds*. 2015;645:535-540.

15. Pacurariu C, Lazau I, Ecsedi Z, Lazau R, Barvinschi P, Marginean G. New synthesis methods of $MgAl_2O_4$ spinel. *Journal of European Ceramics Society*. 2007;27(2-3):707-710.

16. Guo J, Lou H, Zhao H, Wang X, Zheng X. Novel synthesis of high surface area $MgAl_2O_4$ spinel as catalyst support. *Materials Letters*. 2004;58(12-13):1920-1923.

17. Mosayebi Z, Rezaei M, Hadian N, Kordshuli FZ, Meshkani F. Low temperature synthesis of nanocrystalline magnesium aluminate with high surface area by surfactant assisted precipitation method: Effect of preparation conditions. *Materials Research Bulletin*. 2012;47(9):2154-2160.

18. Lee PY, Suematsu H, Yano T, Yatsui K. Synthesis and characterization of nanocrystalline $MgAl_2O_4$ spinel by polymerized complex method. *Journal of Nanoparticle Research*. 2006;8(6):911-917.

19. Abdi MS, Ebadzadeh T, Ghaffari A, Feli M. Synthesis of nano-sized spinel ($MgAl_2O_4$) from short mechanochemically activated chloride precursors and its sintering behavior. *Advanced Powder Technology*. 2015;26(1):175-179.

20. Andeen D, Loeffler L, Padture N, Lange FF. Crystal chemistry of epitaxial ZnO on (111) $MgAl_2O_4$ produced by hydrothermal synthesis. *Journal of Crystal Growth*. 2003;259(1-2):103-109.

21. Fu P, Lu W, Lei W, Wu K, Xu Y, Wu J. Thermal stability and microstructure characterization of $MgAl_2O_4$ nanoparticles synthesized by reverse microemulsion method. *Materials Research*. 2013;16(4):844-849.

22. Ianos R, Lazau I, Pacurariu C, Barvinschi P. Solution combustion synthesis of $MgAl_2O_4$ using fuel mixtures. *Materials Research Bulletin*. 2008;43(12):3408-3415.

23. Padmaraj O, Venkateswarlu M, Satyanarayana N. Structural, electrical and dielectric properties of spinel type $MgAl_2O_4$ nanocrystalline ceramic particles synthesized by the gel-combustion method. *Ceramics International*. 2015;41(2 Pt B):3178-3185.

24. Erukhimovitch V, Mordekoviz Y, Hayun S. Spectroscopy study of ordering in non-stoichiometric magnesium aluminate spinel. *American Mineralogist*. 2015;100(8-9):1744-1751.

25. Mordekovitz Y, Hayun S. On the Effect of Lithium on the Energetics and Thermal Stability of Nano-Sized Nonstoichiometric Magnesium Aluminate Spinel. *Journal of the American Ceramic Society*. 2016;99(8):2786-2794.

26. Halabi M, Ezersky V, Kohn A, Hayun S. Charge distribution in nano-scale grains of magnesium aluminate spinel. *Journal of the American Ceramic Society*. 2017;100(2):800-811.

27. Tripathy S, Bhattachary D. Rapid synthesis and characterization of mesoporous nanocrystalline $MgAl_2O_4$ via ?ash pyrolysis route. *Journal of Asian Ceramic Societies*. 2013;1(4):328-332.

28. Nassar MY, Ahmed IS, Samir I. A novel synthetic route for magnesium aluminate ($MgAl_2O_4$) nanoparticles using sol-gel auto combustion method and their photocatalytic properties. *Spectrochimica Acta Part A: Molecular and Biomolecular Spectroscopy*. 2014;131:329-334.

29. Ganesh I, Srinivas B, Johnson R, Saha BP, Mahajan YR. Effect of fuel type on morphology and reactivity of combustion synthesized $MgAl_2O_4$ powders. *British Ceramic Transactions*. 2002;101(6):247-254.

30. Ganesh I, Johnson R, Rao GVN, Mahajan YR, Madavendra SS, Reddy BM. Microwave-assisted combustion synthesis of nanocrystalline $MgAl_2O_4$ spinel powder. *Ceramics International.* 2005;31(1):67-74.

31. Aruna ST, Mukasyan AS. Combustion synthesis and nanomaterials. *Current Opinion in Solid State and Materials Science*. 2008;12:44-50.

32. Ajamein H, Haghighi M. On the microwave enhanced combustion synthesis of CuO-ZnO-Al_2O_3 nanocatalyst used in methanol steam reforming for fuel cell grade hydrogen production: Effect of microwave irradiation and fuel ratio. *Energy Conversion and Management*. 2016;118:231-242.

33. Rao KJ, Ramesh PD. Use of microwaves for the synthesis and processing of materials. *Bulletin of Materials Science*. 1995;18(4):447-465.

34. Santos AA, Wendler EP, Marques FD, Simonelli F. Microwave-Accelerated Epoxidation of a,ß-Unsaturated Ketones with

Urea-Hydrogen Peroxide. *Letters in Organic Chemistry*. 2004;1:47-49.

35. Lew A, Krutzik PO, Hart ME, Chamberlin AR. Increasing Rates of Reaction:? Microwave-Assisted Organic Synthesis for Combinatorial Chemistry. *Journal of Combinatorial Chemistry*. 2002;4(2):95-105.

36. Kooti M, Sedeh AN. Microwave-Assisted Combustion Synthesis of ZnO Nanoparticles. *Journal of Chemistry*. 2013;2013:562028.

37. Rathi AK, Gawande MB, Zboril R, Varma RS. Microwave-assisted synthesis - Catalytic applications in aqueous media. *Coordination Chemistry Reviews*. 2015;291:68-94.

38. Chang YP, Chang PH, Lee YT, Lee TJ, Lai YH, Chen SY. Morphological and structural evolution of mesoporous calcium aluminate nanocomposites by microwave-assisted synthesis. *Microporous and Mesoporous Materials*. 2014;183:134-142.

39. Bai J, Liu J, Li C, Li G, Du Q. Mixture of fuels approach for solution combustion synthesis of nanoscale $MgAl_2O_4$ powders. *Advances Powder and Technology*. 2011;22(1):72-76.

40. Medeiros RLBA, Macedo HP, Oliveira AAS, Melo VRM, Carvalho AFM, Melo MAF, et al. Síntese de $MgAl_2O_4$ por combustão assistida por micro-ondas: influência dos parâmetros de síntese na formação e na estrutura cristalina. *Cerâmica*. 2016;62(362):191-197.

41. Kiminami RHGA, Morelli MR, Folz DC, Clark DE. Microwave synthesis of alumina powders. *American Ceramic Society Bulletin*. 2000;79:63-67.

42. Tarte P. Infra-red spectra of inorganic aluminates and characteristic vibrational frequencies of AlO_4 tetrahedra and AlO_6 octahedra. *Spectrochimica Acta Part A: Molecular and Biomolecular Spectroscopy*. 1967;23(7):2127-2143.

43. Xie S, Han X, Kuang Q, Zhao Y, Xie Z, Zhen L. Intense and wavelength-tunable photoluminescence from surface functionalized MgO nanocrystal clusters. *Journal of Materials Chemistry*. 2011;21(20):7263-7268.

44. Ewais EMM, Besisa DHA, El-Amir AAM, El-Sheikh SM, Rayan DE. Optical properties of nanocrystalline magnesium aluminate spinel synthesized from industrial wastes. *Journal of Alloys and Compounds*. 2015;649:159-166.

45. Langford JI, Wilson AJC. Sherrer after Sixty Years: A Survey and Some New Results in the Determination of Crystallite Size. *Journal of Applied Crystallography*. 1978;11:102-113.

46. Rashad MM, Zaki ZI, El-Shall H. A novel approach for synthesis of nanocrystalline $MgAl_2O_4$ powders by co-precipitation method. *Journal of Materials Science*. 2009;44(11):2992-2998.

47. Torkian L, Amini MM, Bahrami Z. Synthesis of nano crystalline $MgAl_2O_4$ spinel powder by microwave assisted combustion. *Journal of Inorganic Materials*. 2011;26(5):550-554.

48. Monshi A, Foroughi MR, Monshi MR. Modified Scherrer Equation to Estimate More Accurately Nano-Crystallite Size Using XRD. *World Journal of Nano Science and Engineering*. 2012;2(3):154-160.

49. Wang J, Polleux J, Lim J, Dunn B. Pseudocapacitive Contributions to Electrochemical Energy Storage in TiO_2 (Anatase) Nanoparticles. *The Journal of Physical Chemistry C*. 2007;111(40):14925-14931.

50. Singh AK, Nakate UT. Microwave Synthesis, Characterization, and Photoluminescence Properties of Nanocrystalline Zirconia. *The Scientific World Journal*. 2014;2014:349457.

51. Jiang WT, Peacor DR, Árkai P, Tóth M, Kim JW. TEM and XRD determination of crystallite size and lattice strain as a function of illite crystallinity in pelitic rocks. *Journal of Metamorphic Geology*. 1997;15(2):267-281.